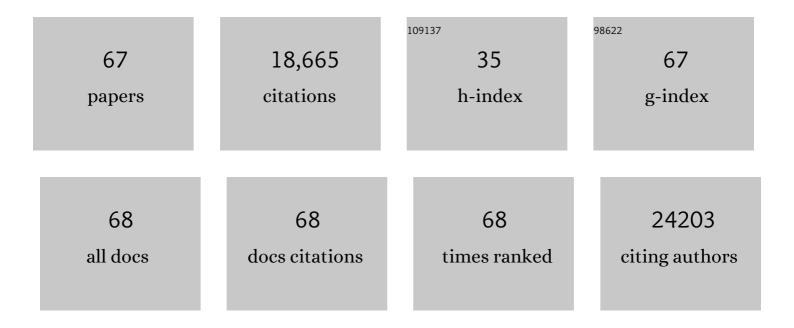
List of Publications by Year in descending order

Source: https://exaly.com/author-pdf/3310606/publications.pdf Version: 2024-02-01



#	Article	IF	CITATIONS
1	Superior Thermal Conductivity of Single-Layer Graphene. Nano Letters, 2008, 8, 902-907.	4.5	11,726
2	Hopping transport through defect-induced localized states in molybdenum disulphide. Nature Communications, 2013, 4, 2642.	5.8	935
3	Robust memristors based on layered two-dimensional materials. Nature Electronics, 2018, 1, 130-136.	13.1	539
4	Integrated digital inverters based on two-dimensional anisotropic ReS2 field-effect transistors. Nature Communications, 2015, 6, 6991.	5.8	505
5	Room temperature high-detectivity mid-infrared photodetectors based on black arsenic phosphorus. Science Advances, 2017, 3, e1700589.	4.7	419
6	Van der Waals epitaxial growth and optoelectronics of large-scale WSe2/SnS2 vertical bilayer p–n junctions. Nature Communications, 2017, 8, 1906.	5.8	369
7	Broadband Photovoltaic Detectors Based on an Atomically Thin Heterostructure. Nano Letters, 2016, 16, 2254-2259.	4.5	322
8	Van der Waals Heterostructures for Highâ€Performance Device Applications: Challenges and Opportunities. Advanced Materials, 2020, 32, e1903800.	11.1	304
9	Unipolar barrier photodetectors based on van der Waals heterostructures. Nature Electronics, 2021, 4, 357-363.	13.1	292
10	High Responsivity Phototransistors Based on Few‣ayer ReS ₂ for Weak Signal Detection. Advanced Functional Materials, 2016, 26, 1938-1944.	7.8	270
11	Gate-tunable negative longitudinal magnetoresistance in the predicted type-II Weyl semimetal WTe2. Nature Communications, 2016, 7, 13142.	5.8	215
12	Gate-tunable van der Waals heterostructure for reconfigurable neural network vision sensor. Science Advances, 2020, 6, eaba6173.	4.7	202
13	Ab initio nonadiabatic molecular dynamics investigations on the excited carriers in condensed matter systems. Wiley Interdisciplinary Reviews: Computational Molecular Science, 2019, 9, e1411.	6.2	194
14	Reconfigurable logic and neuromorphic circuits based on electrically tunable two-dimensional homojunctions. Nature Electronics, 2020, 3, 383-390.	13.1	191
15	Observation of ballistic avalanche phenomena in nanoscale vertical InSe/BP heterostructures. Nature Nanotechnology, 2019, 14, 217-222.	15.6	153
16	Negative Photoconductance in van der Waals Heterostructure-Based Floating Gate Phototransistor. ACS Nano, 2018, 12, 9513-9520.	7.3	124
17	Strain‣ensitive Magnetization Reversal of a van der Waals Magnet. Advanced Materials, 2020, 32, e2004533.	11.1	119
18	Rational Design of α-Fe ₂ O ₃ /Reduced Graphene Oxide Composites: Rapid Detection and Effective Removal of Organic Pollutants. ACS Applied Materials & Interfaces, 2016, 8, 6431-6438.	4.0	91

#	Article	IF	CITATIONS
19	Facile synthesis of iron oxides/reduced graphene oxide composites: application for electromagnetic wave absorption at high temperature. Scientific Reports, 2015, 5, 9298.	1.6	88
20	Sensing Infrared Photons at Room Temperature: From Bulk Materials to Atomic Layers. Small, 2019, 15, e1904396.	5.2	83
21	Gate-Induced Interfacial Superconductivity in 1T-SnSe ₂ . Nano Letters, 2018, 18, 1410-1415.	4.5	81
22	Networking retinomorphic sensor with memristive crossbar for brain-inspired visual perception. National Science Review, 2021, 8, nwaa172.	4.6	77
23	Mono-Elemental Properties of 2D Black Phosphorus Ensure Extended Charge Carrier Lifetimes under Oxidation: Time-Domain Ab Initio Analysis. Journal of Physical Chemistry Letters, 2019, 10, 1083-1091.	2.1	74
24	Experimental Identification of Critical Condition for Drastically Enhancing Thermoelectric Power Factor of Two-Dimensional Layered Materials. Nano Letters, 2018, 18, 7538-7545.	4.5	72
25	A Noble Metal Dichalcogenide for Highâ€Performance Fieldâ€Effect Transistors and Broadband Photodetectors. Advanced Functional Materials, 2020, 30, 1907945.	7.8	72
26	Lowâ€Temperature Eutectic Synthesis of PtTe ₂ with Weak Antilocalization and Controlled Layer Thinning. Advanced Functional Materials, 2018, 28, 1803746.	7.8	70
27	Broadband Bi ₂ O ₂ Se Photodetectors from Infrared to Terahertz. Advanced Functional Materials, 2021, 31, 2009554.	7.8	65
28	Suppression of Electron–Hole Recombination by Intrinsic Defects in 2D Monoelemental Material. Journal of Physical Chemistry Letters, 2019, 10, 6151-6158.	2.1	62
29	Topological transport and atomic tunnelling–clustering dynamics for aged Cu-doped Bi2Te3 crystals. Nature Communications, 2014, 5, 5022.	5.8	60
30	Proximity-Induced Superconductivity with Subgap Anomaly in Type II Weyl Semi-Metal WTe ₂ . Nano Letters, 2018, 18, 7962-7968.	4.5	48
31	Integrated analytical techniques with high sensitivity for studying brain translocation and potential impairment induced by intranasally instilled copper nanoparticles. Toxicology Letters, 2014, 226, 70-80.	0.4	46
32	The preparation of Fe3O4 cube-like nanoparticles via the ethanol reduction of $\hat{1}$ ±-Fe2O3 and the study of its electromagnetic wave absorption. Applied Surface Science, 2015, 359, 723-728.	3.1	46
33	Optimized microstructure and impedance matching for improving the absorbing properties of core-shell C@Fe3C/Fe nanocomposites. Journal of Alloys and Compounds, 2019, 780, 552-557.	2.8	41
34	Controllable SERS performance for the flexible paper-like films of reduced graphene oxide. Applied Surface Science, 2017, 419, 373-381.	3.1	40
35	Tuning Electrical Conductance in Bilayer MoS ₂ through Defect-Mediated Interlayer Chemical Bonding. ACS Nano, 2020, 14, 10265-10275.	7.3	40
36	Direct Evidence for Charge Compensation-Induced Large Magnetoresistance in Thin WTe ₂ . Nano Letters, 2019, 19, 3969-3975.	4.5	37

#	Article	IF	CITATIONS
37	Observation of Negative Terahertz Photoconductivity in Large Area Type-II Dirac Semimetal <mml:math display="inline" xmlns:mml="http://www.w3.org/1998/Math/MathML"><<mml:msub><mml:mrow><mml:mi>PtTe</mml:mi></mml:mrow><mml:mrow><mml:mn>2<td>าl:mn><td>nml:mrow><</td></td></mml:mn></mml:mrow></mml:msub></mml:math>	าl:mn> <td>nml:mrow><</td>	nml:mrow><
38	Nonvolatile van der Waals Heterostructure Phototransistor for Encrypted Optoelectronic Logic Circuit. ACS Nano, 2022, 16, 4528-4535.	7.3	34
39	Gated tuned superconductivity and phonon softening in monolayer and bilayer MoS2. Npj Quantum Materials, 2017, 2, .	1.8	33
40	Robust Impact-Ionization Field-Effect Transistor Based on Nanoscale Vertical Graphene/Black Phosphorus/Indium Selenide Heterostructures. ACS Nano, 2020, 14, 434-441.	7.3	32
41	Hydrothermal growth of TiO2 nanowire membranes sensitized with CdS quantum dots for the enhancement of photocatalytic performance. Nanoscale Research Letters, 2014, 9, 270.	3.1	31
42	Fabrication of Co doped MoS2 nanosheets with enlarged interlayer spacing as efficient and pH-Universal bifunctional electrocatalyst for overall water splitting. Ceramics International, 2021, 47, 24501-24510.	2.3	31
43	WO ₃ and Ag nanoparticle co-sensitized TiO ₂ nanowires: preparation and the enhancement of photocatalytic activity. RSC Advances, 2014, 4, 23831-23837.	1.7	30
44	Plasmon Excited Ultrahot Carriers and Negative Differential Photoresponse in a Vertical Graphene van der Waals Heterostructure. Nano Letters, 2019, 19, 3295-3304.	4.5	28
45	Damage-free and rapid transfer of CVD-grown two-dimensional transition metal dichalcogenides by dissolving sacrificial water-soluble layers. Nanoscale, 2017, 9, 19124-19130.	2.8	27
46	Intrinsic p-type W-based transition metal dichalcogenide by substitutional Ta-doping. Applied Physics Letters, 2017, 111, .	1.5	26
47	Gate-tunable weak antilocalization in a few-layer InSe. Physical Review B, 2018, 98, .	1.1	24
48	Substitutionally Doped MoSe ₂ for Highâ€Performance Electronics and Optoelectronics. Small, 2021, 17, e2102855.	5.2	24
49	Emerging Singleâ€Photon Detectors Based on Lowâ€Dimensional Materials. Small, 2022, 18, e2103963.	5.2	23
50	Microwave absorption of NdFe magnetic powders tuned with impedance matching. Journal of Magnetism and Magnetic Materials, 2018, 449, 385-389.	1.0	22
51	Edgeâ€Epitaxial Growth of InSe Nanowires toward Highâ€Performance Photodetectors. Small, 2020, 16, e1905902.	5.2	22
52	Characterization and photocatalytic activity of (ZnO–CuO)/SBA-15 nanocomposites synthesized by two-solvent method. Materials Research Bulletin, 2014, 56, 119-124.	2.7	21
53	TiO2 nanobelts photocatalysts decorated with Bi2WO6 nanocrystals: Preparation and enhanced photocatalytic activity. Materials Research Bulletin, 2014, 55, 121-125.	2.7	20
54	Enhanced Performance of HgCdTe Midwavelength Infrared Electron Avalanche Photodetectors With Guard Ring Designs. IEEE Transactions on Electron Devices, 2020, 67, 542-546.	1.6	19

#	Article	IF	CITATIONS
55	Gate-tunable ReS2/MoTe2 heterojunction with high-performance photodetection. Optical and Quantum Electronics, 2019, 51, 1.	1.5	15
56	Mesoporous hollow Zn2SiO4:Mn2+ nanospheres: The study of photoluminescence and adsorption properties. Materials Research Bulletin, 2015, 61, 76-82.	2.7	13
57	Topological Phase Transition-Induced Triaxial Vector Magnetoresistance in (Bi _{1–<i>x</i>}) ₂ Se ₃ Nanodevices. ACS Nano, 2018, 12, 1537-1543.	7.3	13
58	Two-solvent method synthesis of SnO2 nanoparticles embedded in SBA-15: Gas-sensing and photocatalytic properties study. Materials Research Bulletin, 2014, 50, 440-445.	2.7	12
59	Ultrafast photocarrier and coherent phonon dynamics in type-II Dirac semimetal PtTe ₂ thin films probed by optical spectroscopy. Photonics Research, 2022, 10, 653.	3.4	12
60	Emerging Lowâ€Dimensional Heterostructure Devices for Neuromorphic Computing. Small Structures, 2022, 3, .	6.9	10
61	A method for the characterization of intra-pixel response of infrared sensor. Optical and Quantum Electronics, 2019, 51, 1.	1.5	8
62	Infrared Gesture Recognition System Based on Near-Sensor Computing. IEEE Electron Device Letters, 2021, 42, 1053-1056.	2.2	8
63	A high-performance quantum well infrared photodetector based on semiconductor–metal periodic microstructure. Optical and Quantum Electronics, 2021, 53, 1.	1.5	8
64	A novel bubbling-assisted exfoliating method preparation of magnetically separable γ- Fe ₂ O ₃ /graphene recyclable photocatalysts. Functional Materials Letters, 2014, 07, 1450056.	0.7	4
65	2 step of conductance fluctuations due to the broken time-reversal symmetry in bulk-insulating BiSbTeSe2 devices. Applied Physics Letters, 2018, 112, .	1.5	3
66	Broadband Photodetectors: Broadband Bi ₂ O ₂ Se Photodetectors from Infrared to Terahertz (Adv. Funct. Mater. 14/2021). Advanced Functional Materials, 2021, 31, 2170093.	7.8	3
67	Preparation and Enhanced Photocatalytic Activity of TiO2 Nanobelts Decorated with Silver Nanoparticles. Asian Journal of Chemistry, 2014, 26, 1341-1345.	0.1	Ο